

Embedded disks in Fornax dwarf elliptical galaxies [★]

S. De Rijcke^{1,★★}, H. Dejonghe¹, W. W. Zeilinger² and G. K. T. Hau³

¹ Sterrenkundig Observatorium, Ghent University, Krijgslaan 281, S9

e-mail: sven.derijcke@rug.ac.be,

e-mail: herwig.dejonghe@rug.ac.be

² Institut für Astronomie, Universität Wien, Türkenschanzstraße 17, A-1180 Wien, Austria

e-mail: zeilinger@astro.univie.ac.at

³ ESO, Alonso de Cordova 3107, Santiago, Chile

e-mail: ghau@eso.org

Received ; accepted

Abstract. We present photometric and kinematic evidence for the presence of stellar disks, seen practically edge-on, in two Fornax dwarf galaxies, FCC204 (dS0(6)) and FCC288 (dS0(7)). This is the first time such structures have been identified in Fornax dwarfs. FCC2088 has only a small bulge and a bright flaring and slightly warped disk that can be traced out to $\pm 23''$ from the center (2.05 kpc for $H_0 = 75$ km/s/Mpc). FCC204's disk can be traced out to $\pm 20''$ (1.78 kpc). This galaxy possesses a large bulge. These results can be compared to the findings of Jerjen *et al.* (2000) and Barazza *et al.* (2002) who discovered nucleated dEs with spiral and bar features in the Virgo Cluster.

Key words. dwarf galaxies – Fornax Cluster – individual galaxies : FCC204, FCC288

1. Introduction

Dwarf ellipticals (dEs) seem to prefer the densest regions of the universe and are found abundantly in galaxy clusters and groups (e.g. Conselice *et al.*, 2001; Ferguson & Sandage, 1989; Binggeli *et al.*, 1987). This circumstance most likely has important consequences for their evolution. Moore *et al.* (1998) have shown how late-type disk galaxies that orbit in a cluster can lose angular momentum by interactions with massive galaxies and, to a lesser degree, by tidal forces induced by the cluster potential. *N*-body simulations performed by Mayer *et al.* (2001) show that small disk galaxies that are close companions to a massive galaxy will be affected likewise. A small disk galaxy is destabilized and develops a bar that gradually slows down by dynamical friction, transporting angular momentum to the halo and to stars at larger radii. Since the latter are being stripped, angular momentum is lost. Gas is funneled in towards the center by torques exerted by the bar where it is converted into stars, thus forming a nucleus. The small companion is heated by the subsequent buckling of the bar (e.g. Merrifield & Kuijken (1999) and references therein) and by bending modes of the disk and is transformed from a rotationally-flattened object into an anisotropic, slowly rotating spheroidal galaxy. The effect on a dwarf galaxy depends on its orbit through a cluster or around a massive companion. For instance, retrograde interactions have a much less damaging effect than prograde ones and may even preserve some of the initial disk structure. Thus, these simulations allow for the existence of fast-rotating dwarfs and for dEs that still contain a stellar disk.

Recently, fast-rotating dEs have been discovered by e.g. De Rijcke *et al.* (2001) and Simien & Prugniel (2002). Jerjen *et al.* (2000) and Barazza *et al.* (2002) discovered spiral structure and bars in 5 bright nucleated dEs in the Virgo Cluster : IC3328, IC0783, IC3349, NGC4431, and IC3468. Ryden *et al.* (1999) also report dEs with disk isophotes in the Virgo cluster. Interpreting small number statistics, about 20% of the Virgo dEs could harbor embedded spiral or bar systems.

In this paper, we present photometric as well as kinematic evidence for the presence of stellar disks in two Fornax dwarf galaxies, FCC204 (dS0(6)) and FCC288 (dS0(7)). In the next section, the photometry of both objects is discussed. In section 3, we present their major-axis stellar kinematics. Our conclusions are summarized in section 4.

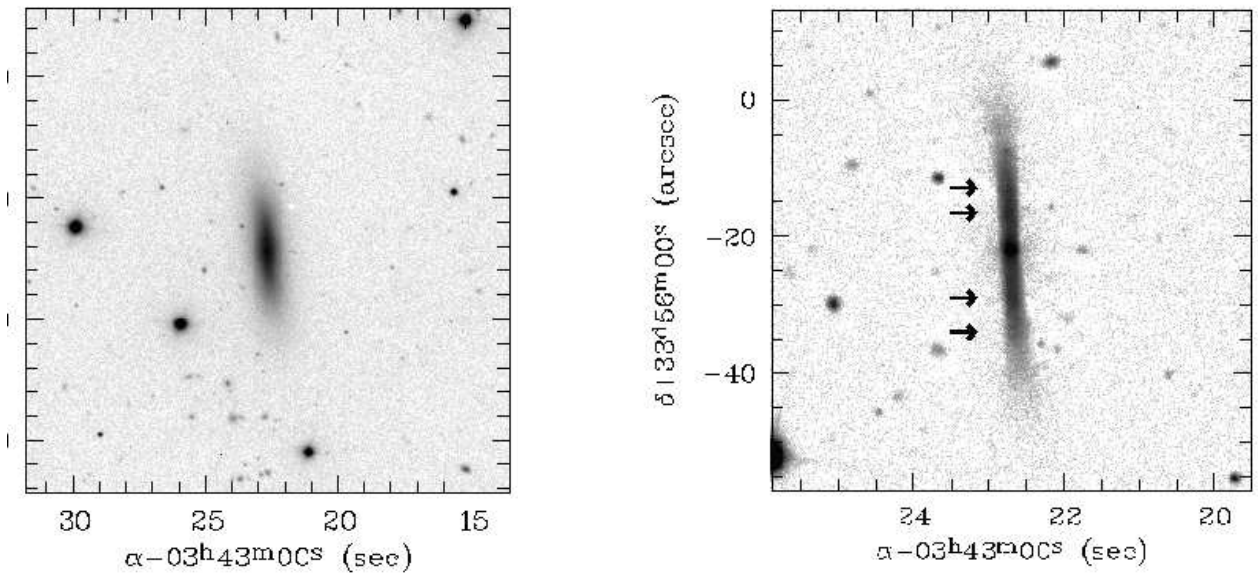


Fig. 1. Left panel : R-band image of FCC288. Right panel : result of unsharp masking. The disk embedded in FCC288 runs practically across the whole face of the galaxy. The flaring of the disk and the brightness fluctuations in it (marked by arrows) are clearly visible. The disk is slightly warped with the north side tending towards the east. The bulge is fairly small, reminiscent of those in late-type spirals.

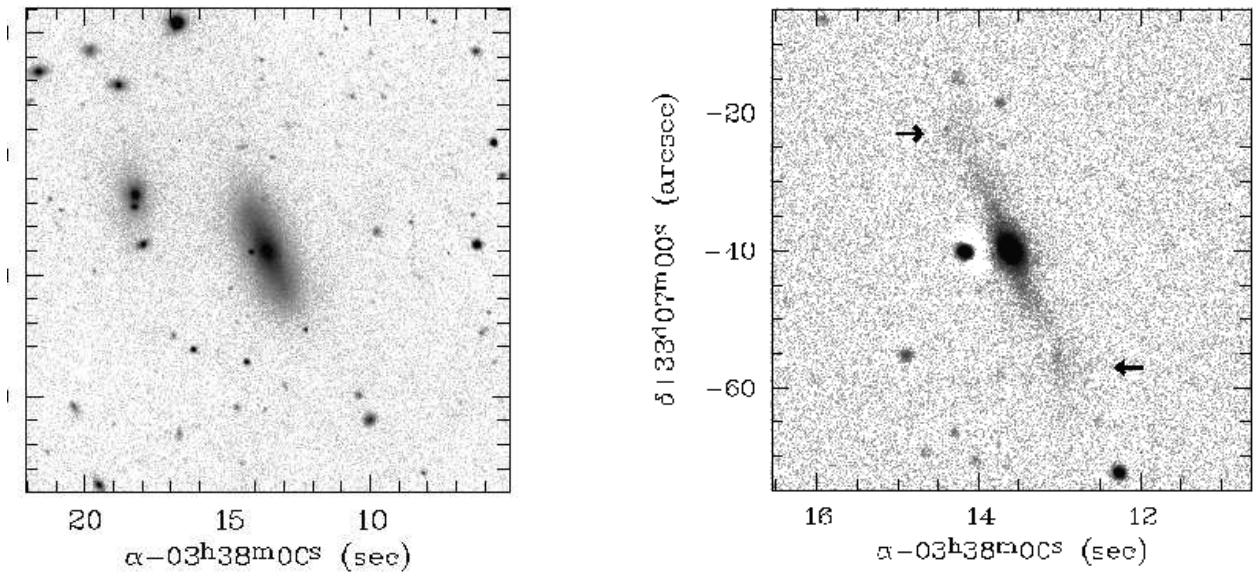


Fig. 2. Left panel : R-band image of FCC204. Right panel : result of unsharp masking. Though much less obvious than in FCC288, a disk can still be discerned. This object has a more massive bulge than FCC288. At the outer edges of the disk, two brightness peaks are visible (marked by arrows).

2. Surface Photometry

We collected R and I band images of a sample of Fornax dEs with FORS2 on Kueyen (VLT-UT2) in the period 1-8/11/2000. The CCD pixel-scale is 0.2". A 600 sec R-band image of FCC288 and a 120 sec R-band image of FCC204 are presented in Figures 1 and 2, respectively. The average seeing was 0.9" FWHM (judged from a number of stars in the R band images) for both galaxies. Basic photometric parameters can be found in Table 1. In Figure 3, the positions of FCC204 and FCC288 are plotted

Send offprint requests to: S. De Rijcke

* Based on observations collected at the European Southern Observatory, Chile (ESO Large Programme Nr. 165.N-0115)
 ** Postdoctoral Fellow of the Fund for Scientific Research - Flanders (Belgium)(F.W.O)

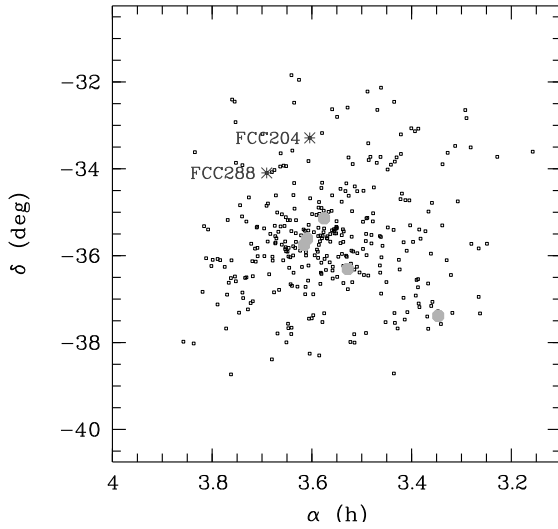
Table 1. Basic photometric and kinematic parameters of FCC204 and FCC288. We used $H_0 = 75$ km/s/Mpc (or equivalently a distance $D = 18.3$ Mpc).

	type	m_B^{0a}	m_R^{0b}	m_I^0	R_e (kpc)	$\langle \epsilon \rangle$	PA ($^\circ$)	n	v_{\max} (km/s)	$\bar{\sigma}$ (km/s)	$(v_{\max}/\bar{\sigma})^*$
FCC204	dS0(6)	14.76	13.88	/	1.03	0.60	21.9	1.29	64.6	56.0	0.75
FCC288	dS0(7)	15.10	14.39	13.86	0.85	0.72	4.6	1.11	60.0	39.9	0.79

^a taken from NED

^b comparison with NED : $m_R^0(\text{FCC288}) = 14.33 \pm 0.9$, $m_R^0(\text{FCC204}) = 13.94 \pm 0.9$

along with all other likely cluster members taken from the Fornax Cluster Catalog (Ferguson 1989). Drinkwater *et al.* (2001) spectroscopically confirmed FCC204 and FCC288 as cluster members. These authors did not detect significant H α emission, corroborating the classification of these galaxies as dS0s and not as dwarf spirals. Both objects are relatively isolated galaxies in the outskirts of the Fornax Cluster, far away from the brightest ($M_B < -20$) Fornax galaxies (the faint galaxy to the east of FCC204 in Figure 2 is FCCB1240, a background elliptical).

**Fig. 3.** Position of FCC204 and FCC288 in the Fornax Cluster (asterisks). The dots mark the positions of all 340 galaxies in the Fornax Cluster Catalog. The brightest cluster members ($M_B < -20$) are plotted as grey dots.

The R- and I-band images were used to extract surface brightness, position angle and ellipticity profiles. The deviations of the isophotes from a pure elliptical shape were quantified by expanding the intensity variation along an isophotal ellipse in a fourth order Fourier series with coefficients S_4 , S_3 , C_4 and C_3 :

$$I(\theta) = I_0 [1 + C_3 \cos(3\theta) + C_4 \cos(4\theta) + S_3 \sin(3\theta) + S_4 \sin(4\theta)]. \quad (1)$$

Here, I_0 is the average intensity of the isophote and the angle θ is measured from the major axis. If the 4th coefficient C_4 is positive, the isophotes are “disky”; otherwise, they are “boxy”. If positive, its value is related to the fractional excess brightness due to the presence of a disk. Else, its value can be related to the fractional brightness decrement at the “tips” of the boxy isophotes. The photometry of all dEs in our sample will be discussed in a forthcoming paper.

The results of this exercise can be found in figure 4, where all photometric quantities are plotted as a function of the geometric mean of the major and minor-axis distances a and b . Both galaxies have positive C_4 profiles, i.e. they have disky isophotes which suggests that they are bulge-disk systems seen practically edge-on. To check whether this diskiness is indeed caused by the presence of a real disk, we applied an unsharp masking technique. We smoothed the R-band image of a galaxy with the MIDAS command `filter/med`¹, which replaces each pixel by the median of a surrounding box. Like Barazza *et al.*, we opted for a $6'' \times 6''$ box. This smoothed image is then subtracted off the original one, highlighting any fine structure. These residual images are presented in the right panels of Figures 1 and 2.

The very prominent disk in FCC288 can be traced out to $\pm 23''$ (2.05 kpc). Clearly visible in Figure 1 is the flaring of the disk, i.e. an increase of the scale-height towards larger radii. The disk is also slightly warped with the north side tending towards the east. We estimated its thickness at a given radial distance from the center by fitting a Gaussian to its vertical profile. The true

¹ ESO-MIDAS is developed and maintained by the European Southern Observatory

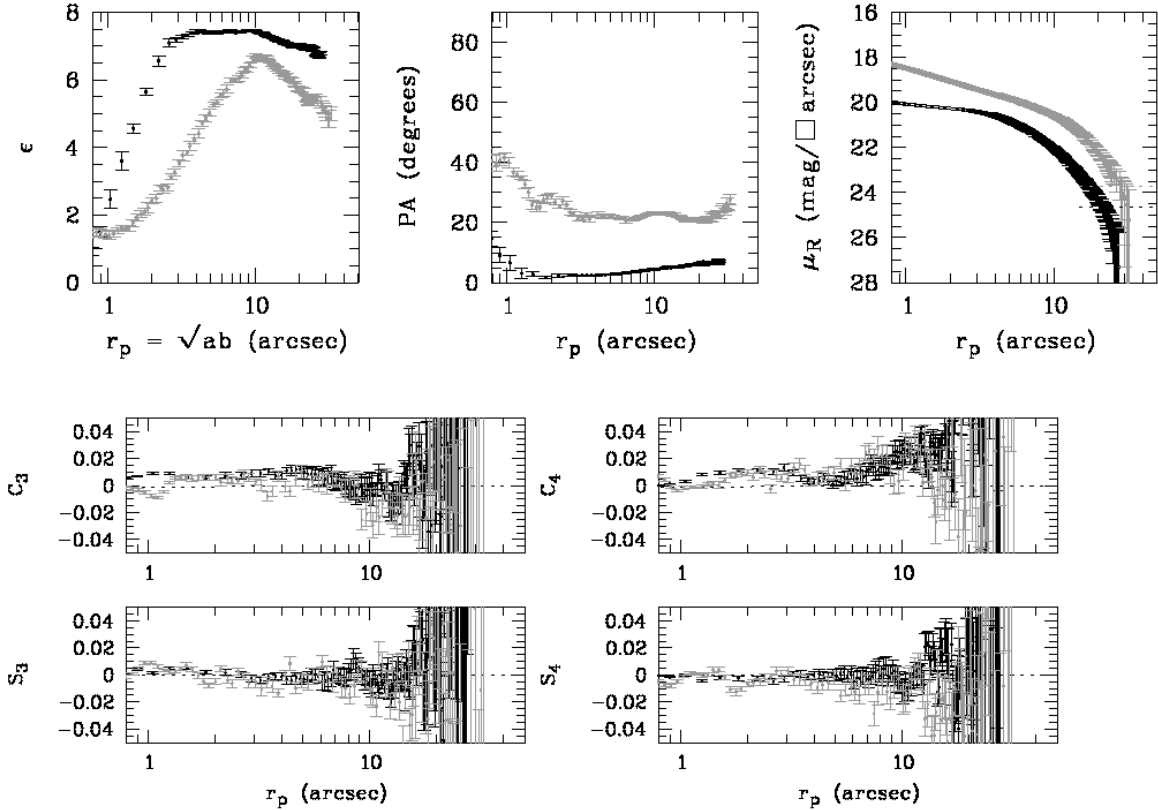


Fig. 4. Photometric parameters of FCC288 (black) and FCC204 (grey) outside the seeing disk. Top row : the ellipticity $\epsilon = 10(1 - b/a)$, the position angle PA and the R-band surface brightness μ_R (the dotted lines mark 1% of the sky intensity). For clarity, the surface brightness of FCC204 has been offset by -1 . Bottom : the third and fourth order shape parameters of the isophotes, S_4 , S_3 , C_4 and C_3 . All quantities are plotted as functions of the geometric mean of the major-axis and minor-axis distances, a and b .

thickness (in a FWHM sense) can be derived from the measured FWHM_{obs} , taking into account the broadening by the seeing using the relation

$$\text{FWHM}_{\text{true}} = \sqrt{\text{FWHM}_{\text{obs}}^2 - \text{FWHM}_{\text{seeing}}^2}.$$

The measured thickness of the disk remains more or less constant around $\text{FWHM}_{\text{obs}} = 2''$ ($\text{FWHM}_{\text{true}} = 160$ pc) inside the inner $10''$. Beyond that, the disk thickens rapidly reaching $\text{FWHM}_{\text{obs}} \approx 6''$ ($\text{FWHM}_{\text{true}} \approx 500$ pc) at a radial distance of $20''$ (Figure 5). In the disk, brightness enhancements can be discerned at $5''$ and $9''$ to the north of the nucleus and at $7''$ and $12''$ to the south of it (marked by arrows in Figure 1). These could signal the presence of spiral arms in the disk.

The vertical scale-height of a disk remains constant only if the vertical velocity dispersion and the surface density drop off in a delicate balance. In the case of an exponential disk with constant M/L , this is quantified by the relation $h_{\sigma_z} = 2h_R$ between the scale-length of the vertical velocity dispersion, h_{σ_z} , and that of the surface brightness, h_R (van der Kruit & Searle, 1981). If this balance is imperfect, the disk will either flare ($h_{\sigma_z} > 2h_R$) or taper ($h_{\sigma_z} < 2h_R$). It is therefore not surprising that flaring optical galaxy disks are not uncommon (see e.g. Narayan & Jog, 2002; Reshetnikov & Combes, 1998). Warped optical disks are discussed by Reshetnikov & Combes (1998). These authors find that about half of all disk galaxies are warped and suggest that tidal interactions have a large influence in creating or re-enforcing warped deformations (see also Weliachew *et al.*, 1978). Bailin & Steinmetz (2002) simulate the reaction of an optical disk to torques exerted by a misaligned dark halo and find that a trailing warp develops. If some dEs stem from harassed disk galaxies, one might expect them to have been stripped of material at large radii – including dark matter – and to have fast dropping surface-densities and consequently to contain flaring disks. The tidal forces exerted on a dwarf galaxy during an encounter can moreover give rise to a warped disk or can induce a misalignment between disk and halo which also yields a warped appearance.

FCC204 has a much less impressive disk, traceable to about $\pm 20''$ (1.78 kpc) and about $3.0''$ thick ($\text{FWHM}_{\text{true}} = 255$ pc). Besides a large bulge, two brightness maxima at $\pm 19''$ from the center are visible (marked by arrows in Figure 2). These might also be signatures of spiral arms. Another possible interpretation is that we are looking edge-on onto a bulge+bar system and that

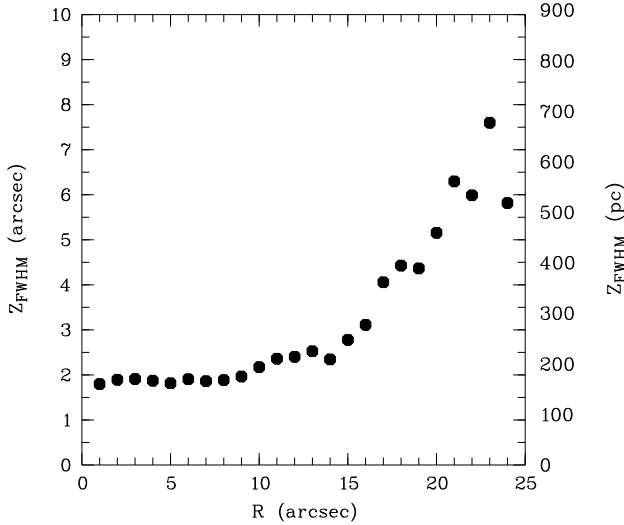


Fig. 5. The vertical thickness ($\text{FWHM}_{\text{true}}$) of the disk embedded in FCC288 as a function of radial distance. On the right side, the corresponding linear distance scale (in parsecs) is added.

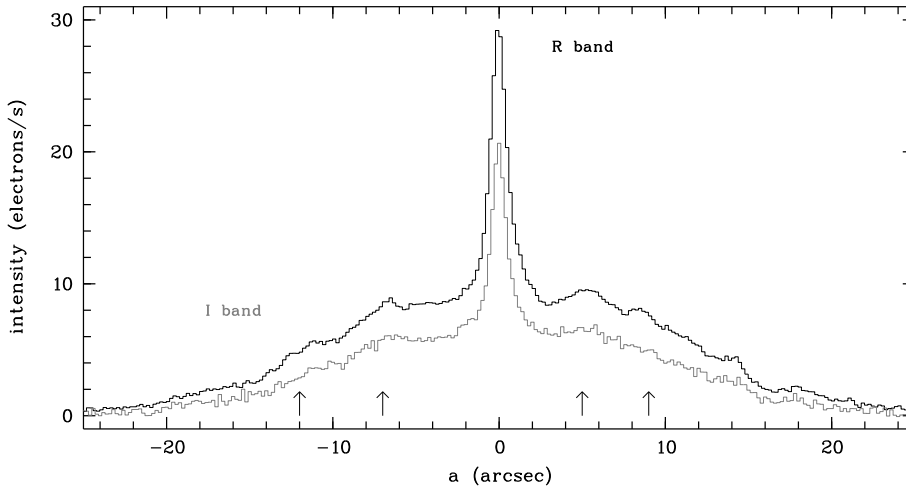


Fig. 6. Cut along the major axis of FCC288, black : R band, grey : I band. Plotted here is the residual of the unsharp masking. The four brightness enhancements are marked with arrows.

the two brightness enhancements, at symmetric positions with respect to the nucleus, constitute the edges of the bar or perhaps are even small spiral arms.

In Figures 6 and 7, we plotted the vertically averaged – i.e. radial – R-band luminosity profiles of the disks in FCC288 and FCC204. Again, one can see the brightness enhancements in FCC288’s disk. Overplotted in Figure 6 is the radial profile of the disk deduced from a 270 sec. I-band image. Although the seeing in the R and I-band images is the same, about $0.9''$ FWHM, the enhancements seem to be less prominent in the I-band image, especially the outer ones. Nevertheless, their showing up also in the I-band image clearly proves that these are not $H\alpha$ emitting gas clouds which would only be visible in the R band.

3. Kinematics

Deep long-slit spectra of FCC288 and FCC204 were obtained with FORS2 in the wavelength region around the CaII triplet during the periods 1-8/11/2000 on Kueyen (VLT-UT2) and 11-21/11/2001 on Yepun (VLT-UT4), respectively. We employed the very efficient holographic grism GRIS_1028z+29 (throughput $\approx 90\%$ around 8500\AA) with a $0.7''$ slit, resulting in an instrumental

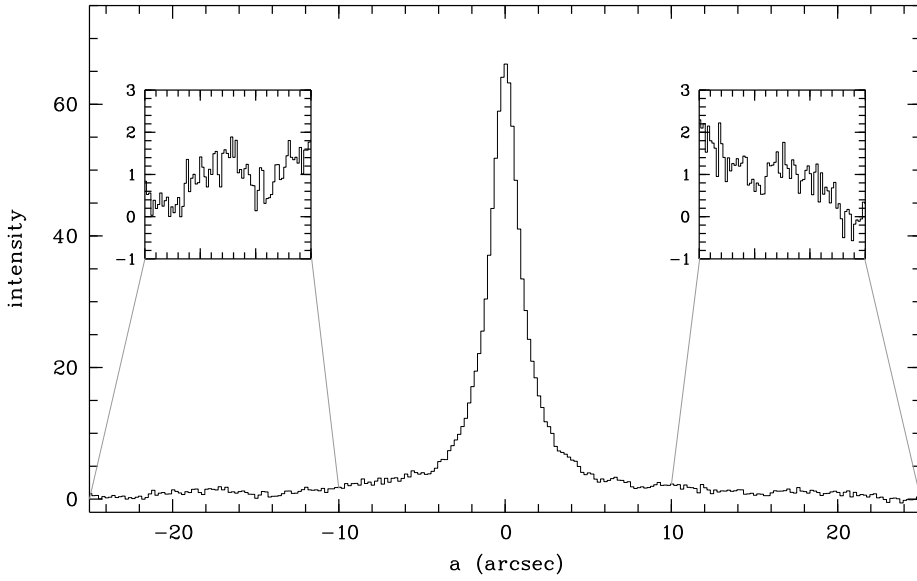


Fig. 7. Cut along the major axis of FCC204. Plotted here is the residual of the unsharp masking. The two insets highlight the brightness enhancements on symmetric positions about the nucleus.

broadening of $\sigma_{\text{instr}} = 30$ km/s. The Doppler broadening of the absorption lines of each row of a galaxy spectrum was modeled with a line-of-sight velocity distribution (LOSVD) of the form

$$\phi(v_p) = \frac{\gamma}{\sqrt{2\pi}\sigma_p} \exp\left(\frac{1}{2}\left(\frac{v_p - \langle v_p \rangle}{\sigma_p}\right)^2\right) \left[1 + h_3 H_3(v_p) + h_4 H_4(v_p)\right] \quad (2)$$

with H_3 and H_4 the third and fourth order Hermite polynomials (van der Marel & Franx, 1993). These take into account asymmetric and symmetric deviations of the LOSVD of a pure Gaussian profile. A positive h_4 yields a LOSVD that is more peaked than a Gaussian whereas a LOSVD with negative h_4 is more flat-topped. A one-dimensional galaxy spectrum can hence be written as the weighted sum of a number of broadened template spectra s_i (typically late GIII to late KIII) and a few low-order polynomials to take into account small differences between the continuum of the galaxy spectrum and that of the sum of broadened stellar spectra :

$$g(\lambda) = \sum_i c_i \int s_i(\lambda(v_p, \lambda)) \phi(v_p) dv_p + \text{continuum}, \quad (3)$$

with $\lambda(v_p, \lambda)$ the wavelength that is Doppler-shifted to λ if a star moves at a velocity v_p along the line of sight. The coefficients c_i are fitted using only the central row of the galaxy spectrum and are kept constant while fitting to the other rows. A quadratic programming technique was used to ensure that the c_i are positive. First, a Gaussian LOSVD is fitted to a 1D galaxy spectrum. The parameters $\langle v_p \rangle$ and σ_p are then kept fixed to fit the coefficients γ , h_3 and h_4 with a simple least-squares technique. It can be shown that the quantities

$$\langle v_p \rangle' = \langle v_p \rangle + \sqrt{3}h_3\sigma_p \quad (4)$$

$$\sigma_p' = \sigma_p(1 + \sqrt{6}h_4) \quad (5)$$

are better approximations of the mean line-of-sight velocity and the velocity dispersion of the LOSVD than the Gaussian estimates. These kinematic parameters are plotted in Figure 8 as a function of position along the major axes of these galaxies. The kinematics of all dEs in our sample will be discussed in a forthcoming paper.

Clearly, both galaxies are very rapid rotators compared to most dwarfs of comparable luminosity. The luminosity-weighted average velocity dispersion of FCC288 is $\sigma_{\text{aver}} = 39.9 \pm 3.9$ km/s, that of FCC204 is $\sigma_{\text{aver}} = 47.0 \pm 5.9$ km/s. The maximum rotation velocities are estimated at $v_{\text{max}} = 60.0 \pm 4.0$ and $v_{\text{max}} = 62.4 \pm 3.6$ for FCC288 and FCC204, respectively. The anisotropy parameter $(v_{\text{max}}/\sigma_{\text{aver}})^*$ is defined as

$$(v_{\text{max}}/\sigma_{\text{aver}})^* = (v_{\text{max}}/\sigma_{\text{aver}})_{\text{obs}} / (v_{\text{max}}/\sigma_{\text{aver}})_{\text{theo}} \quad (6)$$

with $(v_{\text{max}}/\sigma_{\text{aver}})_{\text{obs}}$ the observed ratio and $(v_{\text{max}}/\sigma_{\text{aver}})_{\text{theo}}$ the one expected if the galaxy would be an isotropic, oblate galaxy flattened by rotation. Hence, if a galaxy is flattened purely by rotation, one would expect $(v_{\text{max}}/\sigma_{\text{aver}})^* = 1$. For FCC288, we find

$(v_{\max}/\sigma_{\text{aver}})_{\text{obs}} = 1.50 \pm 0.25$ and FCC204 : $(v_{\max}/\sigma_{\text{aver}})_{\text{obs}} = 1.33 \pm 0.24$. Using equation (4-95) from Binney & Tremaine (1987) to calculate $(v_{\max}/\sigma_{\text{aver}})_{\text{theo}}$, one then finds that $(v_{\max}/\sigma_{\text{aver}})^*(\text{FCC288}) = 0.79 \pm 0.13$ and $(v_{\max}/\sigma_{\text{aver}})^*(\text{FCC204}) = 0.86 \pm 0.16$. Both galaxies have $(v_{\max}/\sigma_{\text{aver}})^* < 1$. This cannot be due to inclination : they are seen practically edge-on. It is most likely due to the fact that the kinematics are influenced by the stars that make up the less flattened (i.e. slower rotating, more anisotropic) body of the galaxy. However, these values are still very high, compared to other dEs. Most dEs observed so far show no or very little rotation (e.g. Geha *et al.* 2002).

Whereas γ , which controls the depth of the absorption lines, h_4 and the velocity dispersion are more or less constant along the major axis of FCC288, they vary significantly inside the inner few arcseconds in the case of FCC204. This is most likely due to presence of the strong bulge in FCC204. The LOSVDs of both disks are quite peaked with $h_4 \approx 0.05$ in the case of FCC288 and $h_4 \approx 0.2$ in that of FCC204. Inside the bulge of FCC204, the LOSVDs have a Gaussian shape. In the disk, the LOSVDs are more peaked and skewed. Beyond about $\pm 20''$, i.e. at the outer edges of the putative bar, the velocity dispersion starts to decline and the rotation velocity levels off. The very fast rotation and the behavior of the various kinematic parameters strengthen our interpretation of the photometrically identified features : both galaxies are seen practically edge-on and contain fast-rotating disk structures. The edges of what we interpret to be a bar in FCC204 correspond with changes in the velocity dispersion and the rotation velocity.

4. Discussion and conclusions

We have presented photometric and kinematic evidence for embedded disks in FCC288 and FCC204, two bright dwarf galaxies in the Fornax Cluster. They were classified as dS0(7) and dS0(6) respectively on the basis of their disk isophotes. These were the only dwarfs that showed any sub-structure out of a sample of 22 dEs (both nucleated and non-nucleated and with a wide variety of ellipticities) from the Fornax Cluster and the NGC5044 and NGC5898 Groups. FCC288 has a very prominent disk, extending to about 2 kpc at either side of the galaxy center, but has only a small bulge, like a late-type disk galaxy. Inside the disk, brightness enhancements can be discerned, which we interpret as traces of spiral arms. The disk flares at larger radii and is slightly warped. FCC204 on the contrary has a large bulge but a much less impressive disk, somewhat like an early-type disk galaxy, extending to about 1.8 kpc, ending in two bright spots on symmetric positions at either side of the bulge. A possible interpretation is that FCC204 contains a bar that ends in two bright knots where small spiral arms start. The kinematic data, particularly the very fast rotation and the correlations between the photometric and the kinematic features, corroborate these interpretations. All observed features can be understood in the context of the galaxy-harassment scenario. If some dEs stem from harassed disk galaxies, they might still contain relics (such as embedded disks) of their former state. The observed flaring and warping of the disk in FCC288 might be consequences of the interactions during the harassment.

Since at the time of writing no dEs with embedded disks were known in other clusters, Barazza *et al.* (2002) noted that Virgo might be somewhat special. It is a very massive and extended cluster (Madore & Freedman, 1998) and galaxies are falling into it at a constant rate (Binggeli *et al.*, 1987). The dEs with embedded disks could then very well be relatively new members of the cluster, distinct from the preexisting dEs, that are currently in the process of being transformed from late-type into early-type dwarfs. Fornax however is less massive and more spatially concentrated than Virgo. Unlike Virgo, it has no continuous infall of galaxies. Therefore, dEs with properties reminiscent of late-type galaxies are most likely formed by harassment of disk galaxies from within the cluster itself. The harassment timescale should then be sufficiently long that they have retained evidence of their original late-type nature.

Acknowledgements. This research has made use of the NASA/IPAC Extragalactic Database (NED) which is operated by the Jet Propulsion Laboratory, California Institute of Technology, under contract with the National Aeronautics and Space Administration. WWZ acknowledges the support of the Austrian Science Fund (project P14783) and of the Bundesministerium für Bildung, Wissenschaft und Kultur.

References

- Bailin J. & Steinmetz M., 2002, astro-ph/0208380
 Barazza F. D., Binggeli B., & Jerjen H., 2002, A&A,
 Binggeli B., Tammann G. A., & Sandage A., 1987, AJ, 94, 251
 Binggeli B. & Cameron L. M., 1993, A&AS, 98, 297
 Binney J. & Tremaine S., 1987, "Galactic dynamics", Princeton University Press, New Jersey
 Conselice C. J., Gallagher J. S. III, & Wyse R. F. G., 2001, ApJ, 559, 791
 De Rijcke S., Dejonghe H., W. W. Zeilinger, & G. K. T. Hau, 2001, ApJ, 559, 21
 Drinkwater M. J., Gregg M. D., Holman B. A & Brown M. J. I, 2001, MNRAS, 326, 1076
 Ferguson H. C., 1989, AJ, 98, 367
 Ferguson H. C. & Sandage A., ApJ, 346, 53
 Geha M., Guhathakurta P., & van der Marel R., 2002, subm. to AJ, astro-ph/0206153
 Jerjen H., Kalnajs A., & Binggeli B., 2000, A&A, 358, 845
 Madore B. F. & Freedman W. L., 1998, "Stellar astrophysics for the local group" : VIII Canary Islands Winter School of Astrophysics, Cambridge University Press, New York

- Mayer L., Governato F., Colpi M., Moore B., Quinn T., Wadsley J., Stadel J., & Lake G., 2001, *ApJ*, 547, 123
Merrifield M. R. & Kuijken K., 1999, *â*, 345L, 47
Moore B., Lake G., & Katz, N., 1998, *ApJ*, 495, 139
Narayan C. A. & Jog C. J., *â*, 390, 35L
Reshetnikov V. & Combes F., 1998, *â*, 337, 9
Ryden B. S., Terndrup D. M., & Pogge R. W., 1999, *ApJ*, 517, 650
Simien F. & Prugniel Ph., *A&A*, 2002, 384, 371
van der Kruit P. C. & Searle L., *â*, 1981, 95, 105
van der Marel R. P. & Franx M., 1993, *ApJ*, 407, 525
Weliachew L., Sancisi R., & Guélin M., 1978, *A&A*, 65, 37

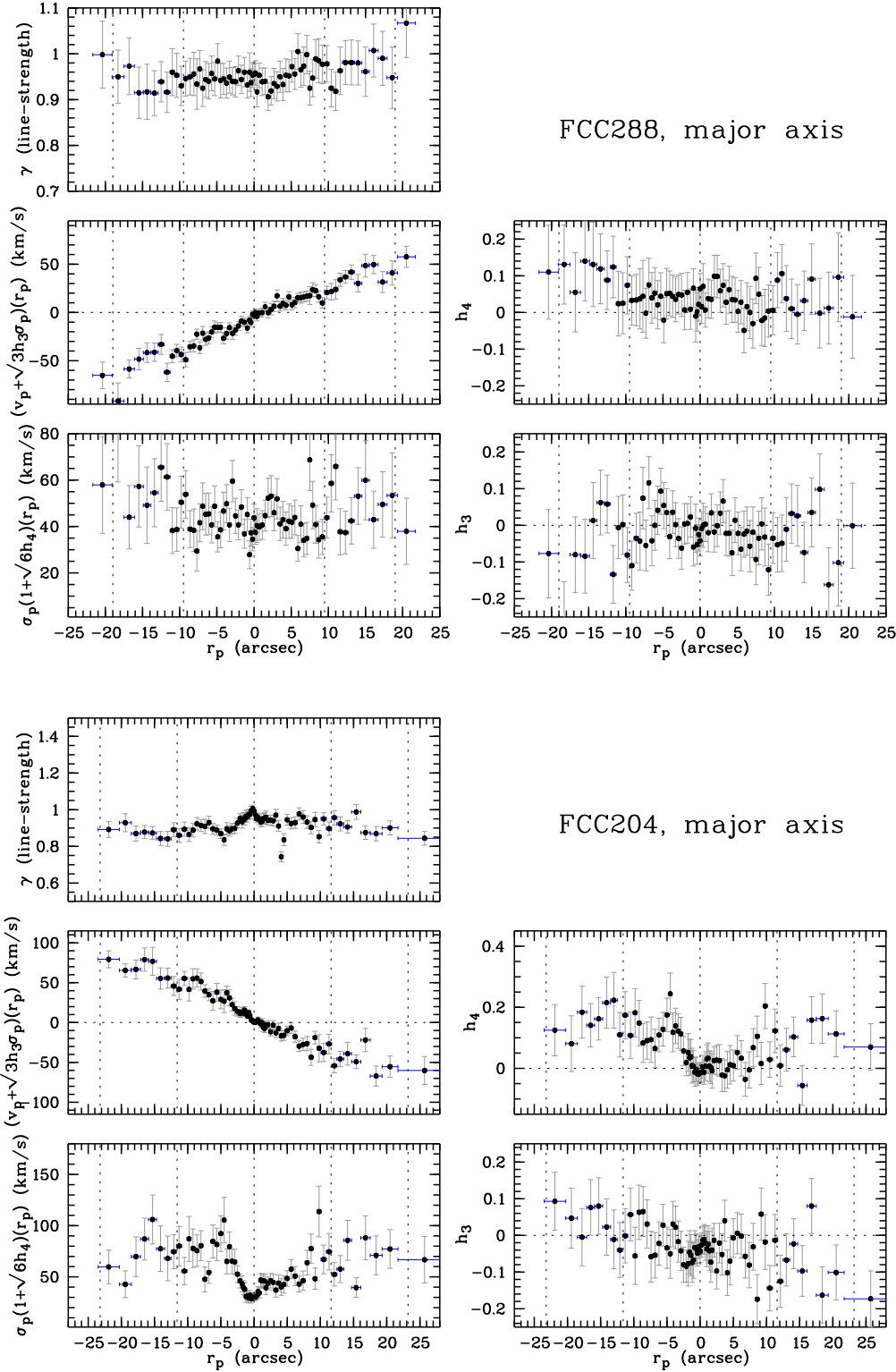


Fig. 8. Major axis kinematics of FCC288 (top) and FCC204 (bottom). For an explanation of these quantities, we refer to the text, section 3. The vertical dotted lines mark ± 1 and ± 2 effective radii.